Synthesis, structural characterization, biological evaluation and of metal complexes with pyrazoline derivatives

J. Joseph[*] and M. Sirajul Muneera

Department of Chemistry, Noorul Islam Centre for Higher Education, Kumaracoil-629180, Tamilnadu

_____

ABSTRACT

A series of novel pyrazoline derivatives have been synthesized by the base-catalyzed Claisen–Schmidt condensation of imidazole-2-carboxaldehyde with 1-acetyl-2-hydroxynaphthalene followed by cyclization with phenylhydrazine (L^1)/ 2,3-dimethylphenylhydrazine (L^2) and 3-nitrophenylhydrazine (L^3). The metal(II) complexes [Ni(II), Co(II), Cu(II) and Zn(II)] were formed by reacting the corresponding metal acetates with the ligands. All complexes were characterized by elemental analyses, electronic, IR, NMR, mass and ESR spectroscopic techniques. The synthesized metal complexes of pyrazoline compounds showed significant antibacterial activity against the organisms Escherichia coli, Staphylococcus aureus, Klebsiella pneumoniae, Proteus mirabillis and Salmonella typhii when compared with the standard antibiotic (Streptomycin). The ligands and their metal complexes were screened for antioxidant activity using DPPH radical scavenging and superoxide radical scavenging assay methods. All the complexes showed good free radical scavenging activity which is comparable to that of the standards. Among the metal complexes, the copper complex has showed higher activity. The results were indicated that 2-pyrazoline (structural core) and copper ion could be responsible for the potential candidate eliciting antioxidant activity. All compounds were evaluated for their in vitro antimycobacterial activity against Mycobacterium tuberculosis. The ligands and metal complexes were subjected to fluorescence properties and exhibited that the variable fluorescence emission behavior of complexes. It can be attributed to the combined effect of the substituents and naphthyl structural core present in the ligands.

Keywords: Antioxidant; Pyrazoline; Standard; Ascorbic acid.

_____

INTRODUCTION

The design of new metal-based chemotherapeutic agent is an emerging research area of inorganic medicinal chemistry [1]. It is well known that medicinal inorganic chemistry is a multidisciplinary field comprises of chemistry, pharmacology, toxicology and biochemistry. The medicinal chemists have focused on design and synthesis of new metal-based molecules with improved biological activity, better selectivity, lower toxicity and multiple role of mechanistic action to overcome the clinical problems of existing drugs in the market due to its side effects. The literature survey demonstrated that the metal complexes are growth inhibitors of microbes and have been extensively studied *in vitro* and *in vivo*.

After the discovery of cisplatin [cis-diamminedichloroplatinum(II)] [2], there has been a rapid developments in inorganic research to find out new and more efficacious metal-based chemotherapeutic drugs [3]. The researchers are motivated and search for new metallic species with improved biological applications. Among the metal ions, copper, nickel, cobalt and zinc complexes have proved to be an excellent candidate [4]. Copper complexes have shown remarkable efficiency in antioxidant [5], DNA-binding and anticancer studies [6, 7]. There is a great deal of interest in the synthesis and characterization of transition metal chelates of heterocyclic compounds, in particular pyrazoline derivatives.

_____

Pyrazoline derivatives are synthetic structural lead molecules of extreme importance for the researchers because of its wide range of biological and pharmaceutical properties such as analgesic, antipyretic and antiandrogenic activities [8, 9]. Pyrazolines have possessed antidepressant, anti-inflammatory and antirheumatic activities [10, 11]. After the pioneering work of Fischer and Knoevenagel in the late nineteenth century, the reaction of α,β-unsaturated aldehydes and ketones and then with hydrazines became one of the most popular methods for the preparation of 2-pyrazolines. 2-Pyrazolines have potential antioxidative effects, capable of preventing oxidative damage as well as clastogenic effects [12, 13]. As a result, numerous substituted 2-pyrazolines have been synthesized.

In recent years, the success of pyrazole moiety as COX-2 inhibitor [14] has highlighted the importance of this heterocycles in medicinal chemistry. A systematic investigation of this class of compounds revealed that pyrazole containing pharmacophore moiety (imidazole) plays an important role in medicinal chemistry. The dominance of pyrazole core in biologically active molecules has stimulated the need for well-designed and efficient ways to make heterocyclic lead for therapeutic purpose.

The interest in compounds of imidazole moiety is due to its unique biological activities [15]. The imidazole ring exists in the histidine and histamine building blocks of proteins, important vitamins (H, B_{12}), alkaloids, and herbicides [16, 17]. The imidazole nucleus occurs in several natural compounds and pharmacologically active substances, displaying a broad range of biological activity [18]. In recent years, it is reported that the incorporation of imidazole nucleus could alter the photophysical as well as the biological properties [19].

It is proposed that the combination of both chemical systems (pyrazoline and imidazole) in one molecule which is required for improved biological activities. This structural core may be a breakthrough for the development of novel lead molecule for antioxidant and antitubercular research work. The various literature reports of pyrazolines [20] and in continuation of our search for new biologically active pyrazoline derivatives [21], we have developed a systematic synthetic approach for the generation of imidazole substituted 2-pyrazoline derivatives.

Structural modifications have been made in the top and bottom of pyrazine moiety (Fig.1) towards the developing of more potent and safer antituberculosis agents. They were carried out in the head and tail portions via substitutions like imidazole and naphthyl moiety. Many of these modified compounds have displayed interesting biological activity, showing that modifications at either site could modulate the activity.

In view of the urgent need of potent and safe antituberculosis agents and in continuation of our earlier interest in this field, here it was planned to synthesize new derivatives by introducing imidazole and naphthyl ring systems at bottom and top of pyrazoline.

According to a literature survey, it was noted that little research work has been carried out on pyrazolines carrying naphthyl/substituted naphthyl groups. Till now, there are no reports on the development of pyrazoline based ligands (incorporation of imidazole and naphthyl moieties) and their transition metal complexes as antituberculosis agents. In view of these facts, we herein described the synthesis and characterization of a pyrazoline based ligands and their Copper(II), Nickel(II), Cobalt(II) and Zinc(II) complexes. Further, the ligands and their metal complexes were subjected to antioxidant and antitubercular activities.

MATERIALS AND METHODS

All the solvents and chemicals used in the synthesis were purchased from commercial suppliers and purified when necessary. The completion of the reaction was monitored by thin layer chromatography and performed on Merck precoated silica gel plates. Silica gel (60–120 mesh size, Merck) was used for column chromatography for purification purpose.

Carbon, hydrogen and nitrogen were estimated by using Elemental Analyzer Carlo Erba EA1108 analyzer. The IR spectrum of synthesized compounds was recorded on a Shimadzu FTIR Affinity-1 Spectrophotometer in the 4000-400 cm^{-1} region in KBr disc. The electronic spectra of the complexes were recorded in HPLC grade DMSO on a Systronics UV-Visible spectrophotometer in the region of 200-1100 nm. The ^{1}H-NMR spectrum of the ligand was recorded in d^{6}-DMSO on a BRUKER 300 MHz spectrometer at room temperature using TMS as an internal reference. FAB-Mass spectra were recorded on a JEOL SX 102/DA-6000 mass spectrometer/data system using Argon/Xenon (6 kV, 10A) as the FAB gas. The accelerating voltage was 10 kV and the spectra were recorded at room temperature and *m*-nitrobenzyl alcohol was used as the matrix. Molar conductivity measurements were recorded on Remi Conductivity Bridge with a cell having cell constant 0.51 and magnetic moment was carried out using Faraday balance. Electrochemical behavior of the metal complexes was investigated with CH Instruments,

_____

U.S.A (Model 1110A-Electrochemical analyzer, Version 4.01) in DMSO containing n-Bu$_4$NClO$_4$ as the supporting electrolyte.

2.1 Synthesis of ligand (L)

A solution of 1-acetyl-2-hydroxynapthalene (0.01 M) and imidazole-2-carboxaldehyde (0.01 M) in 40 ml methanolic NaOH (10% methanolic solution) was stirred well for 6 hrs at room temperature. The solid precipitate was washed with ice-cold water and then rectified spirit, dried. It was recrystallized from ethanol. A mixture of chalcone (0.01 M), phenylhydrazine (0.01 M) L^1/ 2,3-dimethylphenylhydrazine L^2 & 3-nitrophenylhydrazine L^3 and NaOH (0.02 M) was refluxed in 40 mL of methanol for 8 hrs. The solution was poured into ice water which resulted into the precipitation of the ligand (L). The precipitate was filtered and recrystallized from methanol. The recrystallized ligand was dried in a vacuum dessicator over fused calcium chloride.

Ligand (L^1): Molecular formula C22H18N4O, Mol wt. 355. Percentage yield: 68; Elemental analysis: calcd for; C 74.56, H 5.12, N 15.81; Found: C 74.42, H 4.96, N 15.78. UV (nm): 344, 252 nm. FT-IR (KBr disc): 3280 (Ar O–H); 3082-3074 (Ar–H); 2962, 2946, 2932, 2898 (C–H); 1654 (C=N); 1224 (Ar C–OH). ^{1}H-NMR (δ, CDCl$_3$): 3.08 (1H, dd, J = 4.1, 17.6 Hz, 4-Htrans), 3.64 (1H, dd, J = 11.8, 17.6 Hz, 4-Hcis), 5.36 (1H, dd, J = 4.1, 12.1 Hz, 5-H), 6.84-7.56 (m, 11 Ar-H), 10.8 (1H, s, -OH), 7.5 (-CH=CH-, dd, 2H), 8.2 (-CH=CH-, dd, 2H), 12.2 (-NH(imidazole), 1H, s).

Ligand (L^2): Molecular formula C24H22N4O, Mol wt. 382. Percentage yield: 60; Elemental analysis: calcd for; C 74.56, H 5.12, N 15.81; Found: C 74.22, H 4.96, N 15.58. UV (nm): 336, 244 nm. FT-IR (KBr disc): 3342 (Ar O–H); 3092, 3044 (Ar–H); 2948, 2932, 2894 (C–H); 1662 (C=N); 1210 (Ar C–OH). ^{1}H-NMR (δ, CDCl$_3$): 3.16 (1H, dd, J = 4.1, 17.6 Hz, 4-Htrans), 3.48 (1H, dd, J = 11.8, 17.6 Hz, 4-Hcis), 5.54 (1H, dd, J = 4.1, 12.1 Hz, 5-H), 6.76-7.62 (m, 11 Ar-H), 10.6 (1H, s, -OH), 7.4 (-CH=CH-, dd, 2H), 8.0 (-CH=CH-, dd, 2H), 11.8 (-NH(imidazole), 1H, s).

Ligand (L^3): Molecular formula C24H17N5O3, Mol wt. 400. Percentage yield: 56; Elemental analysis: calcd for; C 68.08, H 4.05, N 16.54; Found: C 67.92, H 3.82, N 16.33. UV (nm): 320, 238 nm. FT-IR (KBr disc): 3326 (Ar O–H); 3074, 3042 (Ar–H); 2972, 2944, 2880 (C–H); 1640 (C=N); 1228 (Ar C–OH). ^{1}H-NMR (δ, CDCl$_3$): 3.22 (1H, dd, J = 4.1, 17.6 Hz, 4-Htrans), 3.60 (1H, dd, J = 11.8, 17.6 Hz, 4-Hcis), 5.62 (1H, dd, J = 4.1, 12.1 Hz, 5-H), 6.92-7.76 (m, 11 Ar-H), 11.2 (1H, s, -OH), 7.5 (-CH=CH-, dd, 2H), 8.4 (-CH=CH-, dd, 2H), 12.8 (-NH(imidazole), 1H, s).

Synthesis of complexes

A solution of copper acetate (0.05 M) in 20 mL methanol was added to a stirred solution of ligand (s) (0.05 M) in 20 mL of methanol. The resulting mixture was stirred at room temperature till a precipitate of the complex formed. The precipitate was filtered and washed with cold methanol and hexane. The other metal complexes were prepared using similar procedure. The complexes were dried in a vacuum dessicator over fused calcium chloride.

Copper complex of L^1: Molecular formula C24H22N4O4Cu. Mol wt. 494. Percentage yield: 68; Elemental analysis: calcd for; C 58.36, H 4.49, N 11.34, Cu 12.86; Found: C 58.22, H 4.14, N 11.08, Cu 12.62. UV (nm): 322, 246 & 486 nm. FT-IR (KBr disc): 3331 (Ar O–H); 3080, 3032 (Ar–H); 2956, 2926, 2879 (C–H); 1625 (C=N); 1203 (Ar C–OH). FAB mass spectrometry (FAB-MS): *m/z*: 495 [M+1]. μ$_{eff}$(BM) = 1.88. Λ$_m$ (mhocm^{2}mol^{-1}) = 12.

Nickel complex of L^1: Molecular formula C22H23N4O4Ni. Mol wt. 489. Percentage yield: 72; Elemental analysis: calcd for; C 58.94, H 4.53, N 11.45, Ni 12.00; Found: C 58.72, H 4.30, N 11.36, Ni 11.88. UV (nm): 344, 242, 540 & 739 nm. FT-IR (KBr disc): 3352 (Ar O–H); 3056, 3020 (Ar–H); 2984, 2912, 2870 (C–H); 1630 (C=N); 1214 (Ar C–OH). ^{1}H-NMR (δ, CDCl$_3$): 3.12 (1H, dd, J = 4.1, 17.6 Hz, 4-Htrans), 3.56 (1H, dd, J = 11.8, 17.6 Hz, 4-Hcis), 5.24 (1H, dd, J = 4.1, 12.1 Hz, 5-H), 6.76-7.52 (m, 11 Ar-H), 11.2 (1H, s, -OH), 7.8-7.5 (-CH=CH-, dd, 2H), 12.6 (-NH(imidazole), 1H, s). FAB mass spectrometry (FAB-MS): *m/z*: 490 [M+1]. μ$_{eff}$(BM) = 0. Λ$_m$ (mhocm^{2}mol^{-1}) = 8.

Cobalt complex of L^1: Molecular formula C22H23N4O4Co. Mol wt. 489. Percentage yield: 60; Elemental analysis: calcd for; C 58.91, H 4.53, N 11.45, Co 12.04; Found: C 58.72, H 4.10, N 11.38, Co 11.92. UV (nm): 314, 500 & 645 nm. FT-IR (KBr disc): 3362 (Ar O–H); 3094, 3058(Ar–H); 2962, 2938, 2896 (C–H); 1622 (C=N); 1224 (Ar C–OH). FAB mass spectrometry (FAB-MS): *m/z*: 490 [M+1]. μ$_{eff}$(BM) = 1.75. Λ$_m$ (mhocm^{2}mol^{-1}) = 10.

Zinc complex of L^1: Molecular formula C22H23N4O4Zn. Mol wt. 496. Percentage yield: 72; Elemental analysis: calcd for; C 58.14, H 4.47, N 11.30, Zn 13.19; Found: C 57.96, H 4.22, N 11.08, Zn 12.95. UV (nm): 330, 245, 372 nm. FT-IR (KBr disc): 3384 (Ar O–H); 3072, 3042 (Ar–H); 2962, 2932, 2868 (C–H); 1610 (C=N); 1218 (Ar C–OH). ^{1}H-NMR (δ, CDCl$_3$): 3.24 (1H, dd, J = 4.1, 17.6 Hz, 4-Htrans), 3.72 (1H, dd, J = 11.8, 17.6 Hz, 4-Hcis), 5.56

_____

(1H, dd, J = 4.1, 12.1 Hz, 5-H), 6.92-7.74 (m, 11 Ar-H), 10.6 (1H, s, -OH), 7.9-7.7 (-CH=CH-, dd, 2H), 11.8 (-NH(imidazole), 1H, s). FAB mass spectrometry (FAB-MS): *m/z*: 497 [M+1]. μ_{eff}(BM) = 0. Λ_m (mhocm^{2}mol^{-1}) = 6.

Copper complex of L^2: Molecular formula C26H26N4O4Cu. Mol wt. 522. Percentage yield: 60; Elemental analysis: calcd for; C 59.82, H 5.02, N 10.73, Cu 12.17; Found: C 74.22, H 4.96, N 15.58, Cu 12.04. UV (nm): 322, 246 nm. FT-IR (KBr disc): 3331 (Ar O–H); 3080, 3032 (Ar–H); 2956, 2926, 2879 (C–H); 1645 (C=N); 1203 (Ar C–OH). FAB mass spectrometry (FAB-MS): *m/z*: 523 [M+1]. μ_{eff}(BM) = 1.75. Λ_m (mhocm^{2}mol^{-1}) = 7.

Nickel complex of L^2: Molecular formula C26H26N4O4Ni. Mol wt. 517. Percentage yield: 66; Elemental analysis: calcd for; C 60.38, H 5.07, N 10.83, Ni 11.35; Found: C 74.22, H 4.96, N 15.58, Ni 11.18. UV (nm): 322, 246, 656 nm. FT-IR (KBr disc): 3331 (Ar O–H); 3080, 3032 (Ar–H); 2956, 2926, 2879 (C–H); 1632 (C=N); 1203 (Ar C–OH). ^{1}H-NMR (δ, CDCl$_3$): 3.08 (1H, dd, J = 4.1, 17.6 Hz, 4-Htrans), 3.64 (1H, dd, J = 11.8, 17.6 Hz, 4-Hcis), 5.36 (1H, dd, J = 4.1, 12.1 Hz, 5-H), 6.84-7.56 (m, 11 Ar-H), 10.8 (1H, s, -OH), 7.6-7.7 (-CH=CH-, dd, 2H), 12.2 (-NH(imidazole), 1H, s). FAB mass spectrometry (FAB-MS): *m/z*: 518 [M+1]. μ_{eff}(BM) = 1.75. Λ_m (mhocm^{2}mol^{-1}) = 7.

Cobalt complex of L^2: Molecular formula C26H26N4O4Co. Mol wt. 517. Percentage yield: 64; Elemental analysis: calcd for; C 60.36, H 5.06, N 10.83, Co 11.39; Found: C 74.22, H 4.96, N 15.58, Co 11.16. UV (nm): 322, 246, 644 nm. FT-IR (KBr disc): 3331 (Ar O–H); 3080, 3032 (Ar–H); 2956, 2926, 2879 (C–H); 1624 (C=N); 1203 (Ar C–OH). FAB mass spectrometry (FAB-MS): *m/z*: 518 [M+1]. μ_{eff}(BM) = 1.75. Λ_m (mhocm^{2}mol^{-1}) = 10.

Zinc complex of L^2: Molecular formula C26H26N4O4Zn. Mol wt. 524. Percentage yield: 70; Elemental analysis: calcd for; C 59.61, H 5.00, N 10.69, Zn 12.49; Found: C 74.22, H 4.96, N 15.58, Zn 12.38. UV (nm): 322, 246 nm. FT-IR (KBr disc): 3331 (Ar O–H); 3080, 3032 (Ar–H); 2956, 2926, 2879 (C–H); 1628 (C=N); 1203 (Ar C–OH). ^{1}H-NMR (δ, CDCl$_3$): 3.08 (1H, dd, J = 4.1, 17.6 Hz, 4-Htrans), 3.64 (1H, dd, J = 11.8, 17.6 Hz, 4-Hcis), 5.36 (1H, dd, J = 4.1, 12.1 Hz, 5-H), 6.84-7.56 (m, 11 Ar-H), 10.8 (1H, s, -OH), 7.6-7.7 (-CH=CH-, dd, 2H), 12.2 (-NH(imidazole), 1H, s). FAB mass spectrometry (FAB-MS): *m/z*: 525 [M+1]. μ_{eff}(BM) = 1.75. Λ_m (mhocm^{2}mol^{-1}) = 16.

Copper complex of L^3: Molecular formula C24H21N5O6Cu. Mol wt. 539. Percentage yield: 58; Elemental analysis: calcd for; C 53.49, H 3.93, N 12.99, Cu 11.79; Found: C 53.32, H 3.76, N 12.78, Cu 11.63. UV (nm): 330, 252, 456 nm. FT-IR (KBr disc): 3346 (Ar O–H); 3074, 3062 (Ar–H); 2952, 2946, 2862 (C–H); 1608 (C=N); 1228 (Ar C–OH). FAB mass spectrometry (FAB-MS): *m/z*: 540 [M+1]. μ_{eff}(BM) = 1.94. Λ_m (mhocm^{2}mol^{-1}) = 12.

Nickel complex of L^3: Molecular formula C24H21N5O6Ni. Mol wt. 534. Percentage yield: 64; Elemental analysis: calcd for; C 53.97, H 3.86, N 13.11, Ni 10.99; Found: C 53.72, H 4.04, N 13.02, Ni 10.85. UV (nm): 310, 248 nm. FT-IR (KBr disc): 3324 (Ar O–H); 3092, 3032 (Ar–H); 2956, 2926, 2879 (C–H); 1616 (C=N); 1203 (Ar C–OH). ^{1}H-NMR (δ, CDCl$_3$): 3.16 (1H, dd, J = 4.1, 17.6 Hz, 4-Htrans), 3.72 (1H, dd, J = 11.8, 17.6 Hz, 4-Hcis), 5.42 (1H, dd, J = 4.1, 12.1 Hz, 5-H), 6.90-7.80 (m, 11 Ar-H), 11.2 (1H, s, -OH), 7.8-7.6 (-CH=CH-, dd, 2H), 12.8 (-NH(imidazole), 1H, s). FAB mass spectrometry (FAB-MS): *m/z*: 535 [M+1]. μ_{eff}(BM) =0. Λ_m (mhocm^{2}mol^{-1}) = 10.

Cobalt complex of L^3: Molecular formula C24H21N5O6Co. Mol wt. 534. Percentage yield: 62; Elemental analysis: calcd for; C 53.95, H 3.96, N 13.10, Co 11.03; Found: C 53.74, H 4.06, N 13.02, Co 12.92. UV (nm): 338, 264 nm. FT-IR (KBr disc): 3320 (Ar O–H); 3080, 3048 (Ar–H); 2962, 2946, 2870 (C–H); 1602 (C=N); 1236 (Ar C–OH). FAB mass spectrometry (FAB-MS): *m/z*: 536 [M+1]. μ_{eff}(BM) = 1.84. Λ_m (mhocm^{2}mol^{-1}) = 12.

Zinc complex of L^3: Molecular formula C24H21N5O6Zn. Mol wt. 541. Percentage yield: 60; Elemental analysis: calcd for; C 53.30, H 3.91, N 12.95, Zn 12.09; Found: C 53.02, H 3.96, N 12.84, Zn 11.98. UV (nm): 332, 260 nm. FT-IR (KBr disc): 3368 (Ar O–H); 3092, 3048 (Ar–H); 2964, 2938, 2880 (C–H); 1594 (C=N); 1224 (Ar C–OH). ^{1}H-NMR (δ, CDCl$_3$): 3.18 (1H, dd, J = 4.1, 17.6 Hz, 4-Htrans), 3.72 (1H, dd, J = 11.8, 17.6 Hz, 4-Hcis), 5.46 (1H, dd, J = 4.1, 12.1 Hz, 5-H), 6.92-7.64 (m, 11 Ar-H), 10.4 (1H, s, -OH), 7.7-7.5 (-CH=CH-, dd, 2H), 12.8 (-NH(imidazole), 1H, s). FAB mass spectrometry (FAB-MS): *m/z*: 543 [M+1]. μ_{eff}(BM) = 1.79. Λ_m (mhocm^{2}mol^{-1}) = 8.

DNA Binding Studies

The binding interactions between metal complexes and DNA were studied using electrochemical and electronic absorption methods by using different concentrations of CT-DNA. Calf thymus DNA was stored at 4°C. The DNA stock solutions were prepared with buffer solution (50 mM Tris-HCl at pH 7.2). The stock solutions of the complexes were prepared by dissolving copper complexes in DMSO and diluting with the corresponding buffer to the required concentration for all experiments. This resulted in a series of solutions with varying concentrations of DNA but with a constant concentration of the complex. The absorbance (A) of the most red-shifted band of complex was recorded after each successive additions of CT DNA. The intrinsic binding constant, K_b, was determined from

_____

the plot of [DNA]/(ε_a- ε_f) *vs* [DNA], where [DNA] is the concentration of DNA in base pairs, ε_a, the apparent extinction coefficient which is obtained by calculating A_{obs}/ [complex] and ε_f corresponds to the extinction coefficient of the complex in its free form. The data were fitted to the following equation where ε_b refers to the extinction coefficient of the complex in the fully bound form.

$$[DNA]/(\varepsilon_a- \varepsilon_f) = [DNA]/(\varepsilon_b- \varepsilon_f) + 1/K_b(\varepsilon_b- \varepsilon_f) \text{ -------------- } (1)$$

Each set of data, when fitted to the above equation, gave a straight line with a slope of $1/(\varepsilon_b- \varepsilon_f)$ and a y-intercept of $1/K_b(\varepsilon_b- \varepsilon_f)$. K_b was determined from the ratio of the slope to intercept.

Antioxidant Assay
Superoxide dismutase activity (SOD)
The superoxide dismutase activity (SOD) of the copper complexes were evaluated using alkaline DMSO as source of superoxide radicals ($O_2^{\bullet-}$) generating system in association with nitro blue tetrazolium chloride (NBT) as a scavenger of superoxide. Add 2.1 mL of 0.2 M potassium phosphate buffer (pH 8.6) and 1 ml of 56 μL of NBT solutions to the different concentration of copper complex solution. The mixtures were kept in ice for 15 min and then 1.5 mL of alkaline DMSO solution was added while stirring. The absorbance was monitored at 540 nm against a sample prepared under similar condition except NaOH was absent in DMSO.

Hydrogen peroxide Assay
A solution of hydrogen peroxide (2.0 mM) was prepared in phosphate buffer (0.2 M, 7.4 pH) and its concentration was determined spectrophotometrically from absorption at 230 nm. The complexes of different concentration and vitamin C (100 μg/mL) were added to 3.4 ml of phosphate buffer together with hydrogen peroxide solution (0.6 mL). An identical reaction mixture without the sample was taken as negative control. The absorbance of hydrogen peroxide at 230 nm was determined after 10 min against the blank (phosphate buffer).

Antimicrobial activities
Qualitative determination of antimicrobial activity was done using the well diffusion method. The synthesized Schiff base and its metal complexes were studied for their antibacterial activities in DMSO solvent against bacterial species. The *in vitro* antimicrobial activity was performed against *Escherichia coli, Staphylococcus aureus, Klebsiella pneumoniae, Proteus mirabillis* and *Salmonella typhii,* respectively. The standard and test samples were dissolved in DMSO to give a concentration of 100 μg/mL. The minimum inhibitory concentration (MIC) was determined by serial microdilution method. Dilutions of test and standard compounds were prepared in nutrient broth (bacteria). The samples were incubated at 37 °C for 24 hrs, respectively and the results were recorded in terms of MIC (the lowest concentration of test substance which inhibited the growth of microorganisms). The standard antiobiotic streptomycin and DMSO was used as positive and negative control.

RESULTS AND DISCUSSION

3.1 Chemistry
The researchers have focused on the designing of lead molecules as multifunctional drugs and improving their inhibition activities of Aβ aggregation while retained the main structural core (functional groups) in the lead molecules for their anti-oxidant and metal chelation properties. In the present study, most of the designed compounds contain naphthyl core for their anti-oxidant activities. From the literature facts, we know that the aromatic groups and polar substitution are essential to their pharmacological activities in terms of the efficient binding at the Aβ peptide guided by π-stacking and hydrogen bonding interactions. Therefore, the structural moieties are responsible for their biological activities.

Keeping these facts in mind, the synthesis of novel series of pyrazoline derivatives (L[1], L[2] & L[3]) and their reaction sequence are outlined in scheme 1. The chalcones (1-3) were prepared by base catalyzed Claisen-Schmidt condensation of 1-acetyl-2-hydroxynaphathalene and imidazole-2-carboxaldehyde in the presence of base. The cyclization of chalcone with substituted phenylhydrazine under basic condition leads to the formation of new 2-pyrazoline derivatives. These compounds were used as ligands to prepare metal(II) complexes [ML(OAc)(H_2O)] by mixing an equimolar ratio of ligand with metal acetate(s) refluxed in methanol (Scheme 1).

The analytical data of the ligands and their metal(II) complex were summarized in the experimental section. They are well agreed with the theoretical values within the limit of experimental error. The metal complexes are quite stable in air & light. They are soluble in most of the common organic solvents. The structure of ligands and their metal complexes were established using elemental analyses, IR, UV, NMR, electronic spectra, FAB-MS and thermo gravimetric analysis.

_____

3.2 Molar conductance measurements

Molar conductance measurements of metal complexes were carried out in DMSO at room temperature. Molar conductance values for 10^{-3}M solutions of copper, nickel cobalt and zinc complexes in DMSO were found in the range of 6-14 Ω^{-1} cm^2 mol^{-1}, respectively. These values are in good accordance with the non-electrolytic nature of the complexes [22].

3.3 IR spectra

The important bands of the IR spectra of 2-pyrazoline derivatives (L[1], L[2] & L[3]) and their metal complexes are summarized in the experimental section. There is a appearance of strong stretching band at 1634 cm^{-1} due to α,β-unsaturated (C=O) group. It was confirmed by the condensation of 1-acetyl-2-hydroxynaphthalene with imidazole-2-carboxaldehyde. Furthermore, the absence of stretching frequency of α,β-unsaturated (C=O) and the presence of (C=N) and (C-N) stretching frequencies at 1596 and 1244 cm^{-1} in the IR spectrum of the ligand (experimental section) was confirmed the cyclization of chalcone with substituted phenylhydrazine to form the pyrazoline derivatives as ligands (L[1], L[2] & L[3]). The IR spectra of the complexes showed a strong band in the region 1662–1640 cm^{-1} which are assignable to the ν(C=N) stretch and shift of this band (20–48 cm^{-1}) to lower frequency indicates the involvement of azomethine nitrogen in coordination. The compounds (L[1], L[2] & L[3]) showed additional sharp bands in the region 3312–3438 cm^{-1} due to the ν(NH) stretch of imidazole moiety. A band at 1359 cm^{-1} was assigned to the vibration frequency of the phenolic C–O group. In the complexes, the band assigned to the vibration frequency of the phenolic C–O group undergoes positive shifts, indicating that the Schiff base is bonded to the metallic ions through the phenolic oxygen atoms [23, 24]. The IR spectra of all the complexes show new absorption bands in the region 3300-3500 cm^{-1} indicating the presence of water molecules. In addition, the band at 860 cm^{-1} in the IR spectra of Co(II) and Ni(II) complexes suggests that water molecules are coordinated to metal ions [25]. Therefore, the proposed coordination sites for the synthesized ligands are azomethine nitrogen and hydroxyl oxygen atoms, respectively. The synthesized ligands are behaved as bidentate manner. The IR spectra of all the complexes showed two absorption bands in the far infrared region, 420-440 cm^{-1} and 480-520 cm^{-1}, which are assignable to υ(M-O) and υ(M-N) vibrations, respectively. Further, the υ(asym) and υ(sym) vibrational bands for acetate in the complex were appeared at 1510 and 1400 cm^{-1}. The difference is ~110 cm^{-1} indicates that acetate ion bound as monodentate fashion. The IR spectrum of copper complex of L[2] was shown in fig.2.

3.4 Electronic absorption spectra

The absorption spectral data of the compounds in DMSO are presented in the experimental section. In the electronic absorption spectrum of ligand (L[1]), the bands are observed at 344 and 252 nm which may be assignable to n-π* and π- π* transitions, respectively. The band was observed at 344 nm which is assignable to the transition involving the azomethine moiety (C=N) of pyrazoline structural core. The other absorption bands at 252 nm is due to π- π* transition of phenyl ring. These transitions were slightly shifted towards lower wavelengths due to coordinating effect of the metal ions. The electronic spectrum of the copper complex exhibits bands at 486 nm which can be assigned to $^2B_{1g} \rightarrow ^2A_{1g}$ transition [26]. The square-planar geometry of Cu(II) ion in the complex is confirmed by the measured magnetic moments values, 1.88 B.M. The square-planar geometry is achieved by the coordination of HL as bidentate ligand, to the copper(II) ion.

The electronic spectrum of the nickel complex of L[1] showed the two bands at 540 and 739 nm which are attributed to $^1A_{1g} \rightarrow ^1A_{2g}$ and $^1A_{1g} \rightarrow ^1B_{2g}$ transitions, respectively [26]. These transitions, as well as the measured value of the magnetic moment (μ_{eff} = 0) suggest a square-planar geometry of the complexes. In the case of Co(II) complex of L[1], square planar Co(II) complexes exhibit two bands around 645 and 500 nm which corresponds to the transitions $^2A_{2g} \rightarrow ^2B_{1g}$ and $^2A_{1g} \rightarrow ^2E_g$, respectively [25]. It has showed a μ_{eff} value is 2.18 BM which corresponds to one unpaired electron for square planar geometry. The Zinc(II) complex does not exhibit d–d electronic transition due to the completely filled d-orbital. It exhibits the absorption at 372 nm could be assigned to a charge transfer transition. Similarly, all the other complexes showed spectral features and are summarized in the experimental section.

3.4.1 Stability of metal complexes in buffer medium

DNA interactions have been performed in Tris–HCl/NaCl buffer. It is necessary to check the stability of metal complexes in this buffer medium. The UV–Vis., spectral study was performed under conditions similar to those used for DNA binding studies. The spectral features of the complexes exhibited no change in the position of absorption bands over a period of 48 hrs and no precipitation or turbidity was observed even after long storage at room temperature (at least 1 month after preparation). This suggests that the Cu(II) complexes are completely stable under the experimental conditions.

3.5 Metal-chelating properties of Pyrazoline derivatives

Alzheimer's disease (AD), a progressive neurodegenerative brain disorder, is affecting more and more elderly all around the world [27, 28]. Firstly, abnormal enrichment of Cu, Fe, and Zn in postmortem AD brain has been

_____

confirmed [29]. In vitro experiments revealed that these metals are able to bind to Aβ, thus promoting its aggregation [30]. On the other hand, redox-active metal ions like Cu and Fe contribute to the production of ROS and widespread oxidation damages observed in AD brains [31, 32]. Therefore, removal of biometals in the brain provides a potential therapeutic strategy for the treatment of AD. In the present study, the metal chelation property of synthesized pyrazoline derivatives may be inhibiting Aβ aggregation in brain.

The chelation tendency of pyrazoline derivatives with biometals (Cu, Co, Ni & Zn) was performed by electronic absorption technique. The electronic absorption spectrum of pyrazoline (L^1) in DMSO showed peaks at 252 and 344 nm. The addition of copper acetate, there is a red shift in the absorption peak and new peaks were also observed. The peaks are observed at 246, 322 (red shift) and 486 nm (d-d transition) which corresponds to the formation of complex. Therefore, pyrazoline derivatives had the ability to form complexes with metal salts. The stoichiometry of the complex formation was ascertained from the elemental analysis and molar conductance studies. The molar conductance values are lower in accordance with non electrolytic nature of complexes. The structural core and various substituents are responsible for the complexation with metal ions. It is acquired that the important property of pyrazoline derivatives acting as metal chelator.

The observed results strongly encourage further structural and biological optimization of pyrazoline derivatives to develop as more potent and safer lead molecules for anti-Alzheimer agents.

3.6 ^{1}HNMR spectra

The structures of ligands and their nickel and zinc complexes were recorded in DMSO as solvent and TMS as internal standard. The chemical shifts of characteristic protons in these compounds are expressed in ppm and summarized in the experimental section. ^{1}H-NMR spectra of ligands exhibited an AMX pattern for the presence of two diastereotopic protons at C-4 and one single proton at C-5 positions in the pyrazoline ring. These protons are appeared as three doublet of doublets in the ligand L^1. They are observed in the δ = 3.25-3.64, 3.92-4.67 and 5.31-6.28 ppm regions, each integrating for one proton. The weak signal was observed at 12.2 ppm which is assigned to the deshielded proton of phenolic –OH [33]. There is no signal was observed in the nickel and zinc complexes. It implies that the phenolic oxygen atom is involved in coordination. The most downfield signals was observed as a singlet at 10.8 ppm due to NH proton of imidizole moiety which is D_2O exchangeable. The two more doublet of doublet was observed at 7.5 and 8.2 ppm which corresponds to –CH=CH-. The aromatic protons are appeared around 6.84-7.56 ppm in the ligand L^1. In the case of nickel and zinc complexes, there is a small downfield shift was observed in the protons.

The ^{13}C NMR spectra of all the compounds showed the signals in the respective regions. The azomethine carbon of the pyrazoline ring was observed in the ligands at 152.8-158.6 pm. The signals in the range 118.20-148.50 ppm were observed in the spectra of all the compounds due to the aromatic carbons. The carbons, C4 and C5 positions, of the pyrazoline ring resonated at 64.38-68.28 and 48.34-49.50 ppm in the ligands. Further, there is slight downfield shifted signal was observed which may be attributed to metal coordination.

3.7 Mass spectra

The mass spectra of the title compounds exhibited molecular ion peaks at their respective molecular weights which confirmed their formation. The characteristic peaks were observed in the mass spectra of ligands and their metal complexes. The mass spectrum of ligand L^1 showed a molecular ion peak at m/z 355 which might be due to total molecular weight of the ligand. Mass spectrum of [CuL^1(OAc)(H$_2$O)] showed a molecular ion peak at 497. The molecular ion peak (M$^+$) for all the compounds was observed at their respective molecular masses, fragmentation pattern was also in good agreement with already reported 2-pyrazoline derivatives [34-37]. The molecular mass data of all the synthesized pyrazoline derivatives and their metal complexes are provided in the experimental part.

3.8 ESR Spectra

The EPR spectrum of Cu(II) complexes were recorded at RT and LNT. They were exhibited four peaks with an axial symmetry (g_{II} = 2.2252-2.2346, $g_\perp$ = 2.0946-2.1260, A_{II}=162-148 G) which is associated with square planar coordination around copper(II) ions. Diaz et al. had studied and summarized a good correlation between 'f' factor (g_{II} / A_{II}, where A_{II} is expressed in cm^{-1}) and SOD activity of copper(II) complexes [38]. The 'f' factor value smaller than 135 cm is obtained for square planar Cu(II) complexes, and this value increases with increasing tetrahedral distortion. The 'f' value for Cu, Zn SOD is 160 cm, indicating a tetrahedral distortion from square planar geometry and is one of the features that enhance the catalytic activity of the enzyme. From the above EPR data the f values for copper complexes were determined to be 150-158 (g_{II} / A_{II}). Therefore, the synthesized Cu(II) complexes exhibiting appreciable square planar distortion is expected to show high SOD-like activity.

_____

3.9 Thermogravimetric analysis

Thermogram of metal complexes was recorded under nitrogen atmosphere with a heating rate of 10 °C min^{-1} between room temperature 0°C to 800 °C. All the complexes were stable up to 150°C. Further increment of temperature causes decomposition of the complexes in three steps. The temperature range for the first step was 150–187°C which is corresponds to removal of coordinated water molecule. The second decomposition step was assigned to the loss of acetate ion in the metal complexes. The third step starts immediately after the second step and continues until the complete decomposition of the ligand and formation of the end product as metal oxide. The total weight loss of the complexes corresponds to the loss of respective ligands after considering the transfer of one oxygen atom to the metal ion and the residue corresponds to the metal oxide.

4.   Biological screening
4.1 DNA binding studies
4.1.1 Electronic absorption method

DNA-binding studies are important for the rational design and construction of new and more efficient drugs targeted to DNA [39]. A variety of small molecules interact reversibly with double-stranded DNA, primarily through three modes: (i) electrostatic interactions with the negativecharged nucleic sugar–phosphate structure, which are along the external DNA double helix and do not possess selectivity; (ii) binding interactions with two grooves of DNA double helix; and (iii) intercalation between the stacked base pairs of native DNA. Heterocyclic molecules interact through intercalation with the planar, aromatic group stacked between base pairs [40–42]. In order to explore the mode of the Cu(II) complex binding to DNA, the experiments have been carried out as follows:

Electronic absorption spectroscopy is an effective method to find out the binding mode of DNA with metal complexes. ''Hyperchromic effect'' and ''hypochromic effect'' are the spectra features of DNA concerning its double-helix structure with molecules[43]. This spectral change reflects the corresponding changes of DNA in its conformation and structures after the molecule bound to DNA. Hypochromism results from the contraction of DNA in the helix axis, as well as from the change in conformation on DNA, while hyperchromism results from the damage of the DNA double helix structure [43].

In general, a compound binding to DNA through intercalation usually results in hypochromism with or without a small red or blue shift, due to the intercalation mode involving a strong stacking interaction between the planar aromatic chromophore and the base pairs of DNA [44]. The extent of hypochromism is commonly consistent with the strength of the intercalative binding interaction. More than one type of DNA-compound interactions have been formed (partial intercalation + electrostatic attraction) as indicated by the absence of any fixed isobestic points in titration experiment.

The metal(II) complex can bind to the double stranded DNA in different binding modes on the basis of their structure, charge and type of ligands. As DNA double helix possesses many hydrogen bonding sites which are accessible both in the minor and major grooves, it is likely that the –OH group of L-tyrosine ligand in the metal(II) complex form hydrogen bonds with DNA, which may contribute the hypochromism observed in the absorption spectra.

The absorption spectrum of copper complex of Ligand (L^3) in the absence and presence of CT-DNA are shown in Fig. 3. Upon incremental addition of DNA, the absorption band of the ligand exhibits a hypochromism of about 21.80% with a blue shift of 4 nm corresponding to the absorbance at 332 nm, whereas the absorption band of the copper(II) complex at 344 nm exhibits the same phenomenon of hypochromism of about 58% with a blue shift of about 5 nm. These spectral characteristics revealed that both the ligand and complex interact with CT-DNA most likely through an interaction mode that involves stacking interaction between the aromatic chromophore and the base pairs of DNA. The copper complex showed more hypochromicity than the ligand, indicating that the binding strength of the copper(II) complex is stronger than that of the free ligand.

Further, in the case of copper complexes, there is a change in absorbance and shift in wavelength (blue shift) in the visible absorption region which corresponds to the possibility of copper ion interacts with N^7-guanine nitrogen atom in base pair. It is concluded that copper complexes exhibited higher binding strength than other metal complexes under the study.

The higher hypochromism and K$_b$ value obtained for copper complex of L^2 suggest its higher binding affinity to DNA than that for other complexes. This may be due to the presence of methyl group on phenyl ring which is involved in hydrophobic interaction with the hydrophobic DNA surface that leads to enhancement of DNA binding affinity. The observed less binding affinity of complex may be due to the presence of methyl group when compared to NO$_2$ present in complex of L^3, which disturb the intercalation of DNA base pairs.

_____

Additionally, hydrogen bonding is also possible in the interaction of DNA with complexes. DNA possesses several hydrogen bonding sites in major as well as minor grooves, and complexes contain -NH groups, there could be hydrogen bonding between the complexes and the base pairs in DNA [45].

4.1.2 Electrochemical study

Cyclic voltammetry is a versatile tool in the study of DNA interaction with redox active molecules. It may yield information about the interaction mode with both oxidized and reduced form of the metal ion. In general, when the metal complex binds to DNA via intercalation, the electrode potential shows a positive shift while in the case of electrostatic interaction, the potential will shift to a negative direction. If more than one potential exist simultaneously, a positive and negative shift of electrode potential, the molecule may bind to DNA by both intercalation and electrostatic interaction [46].

In the present study, the DNA binding efficiencies of metal complexes were performed using cyclic voltammetry (CV) in DMSO as solvent (Fig. 4), using a three-electrode cell consisting of a glassy carbon working electrode, a platinum wire auxiliary electrode and standard calomel electrode (SCE) as the reference electrode with a scan rate of 100 mV s^{-1}. The interaction of metal complexes with DNA has been also investigated by monitoring the changes observed in the cyclic voltammogram of a 0.25 mM/ buffer solution of the complexes upon addition of DNA. The buffer was also used as the supporting electrolyte.

Generally, the copper complexes produce redox signal because of the strong and easy electron donation-acceptance properties between Cu^+ and Cu^{2+}. The cyclic voltammograms of the Cu(II) complex of L^1 in the absence and presence of DNA in a Tris/NaCl buffer solution in the range +1.6 to -1.2 V with a scan rate of 100 mV/s. In the absence of DNA, it shows a quasi-reversible one electron redox process involving the Cu^{2+}/Cu^+ couple [Epc at +946 mV and Epa at + 864 mV]. The E1/2 was taken as the average of Epc and Epa is +82 mV in the absence of DNA. In the presence of DNA, the cathodic peak potential (Epc) appears at +932 mV and the anodic peak potential (Epa) at +856 mV. The $E_{1/2}$ is +76 mV in the presence of DNA. In the presence of DNA, both anodic and cathodic peak potentials were shifted to more positive values implying that L^1 bind to DNA by intercalation. The current intensity of peaks decreased significantly, suggesting the existence of an interaction between the complexes and DNA. The reduction in the cathodic and anodic peak currents due to slow diffusion of an equilibrium mixture of the free and DNA bound complex to the electrode surface [47]. Similar behavior was also observed with increased DNA concentration and scan speed and the voltammetric current also decreased as expected for intercalative binding.

4.2 Antioxidant

The metal complexes of pyrazoline derivatives were subjected for their evaluation of antioxidant activities using DPPH radical scavenging assay and superoxide scavenging assay methods. After systematic evaluation of DPPH assay and superoxide scavenging assay, it is revealed that cobalt, nickel, copper and zinc complexes have shown the potential antioxidant activity. Among the metal complexes, the copper complex of L^2 is the best molecule when compared with ascorbic acid. It signifies the role of electron releasing group CH_3 at 2, 3-disubstituted group of 2-pyrazoline for the inhibition of free radicals. Electron withdrawing group reduce the efficiency of hydrogen release from the amino group of imidzole moiety in the pyrazoline scaffold. In the case of nitro substituent on the 3-phenyl hydrazine of pyrazoline, the antioxidant activity is greatly reduced. It is revealed that the nitro substituent of pyrazoline derivative is not recommended for antioxidants.

Hydroxyl radical is highly reactive oxygen centered radical formed from the reactions of various hydroperoxides with transition metal ions [48]. Hydroxyl radical is known to be capable of abstracting hydrogen atoms from membrane lipids and brings about peroxide reaction of lipids. The antioxidant activity of free ligand, complexes and the standard ascorbic acid were assessed on the basis of the radical scavenging effect of the stable DPPH (1,1-diphenyl-2-picryl hydrazyl) free radical. The results were summarized in table 1. The comparision of the antioxidant activity of the ligand (IC_{50} value is 86 µg/mL) with that of the metal complexes (IC_{50} values of Cu(II), Ni(II), Co(II) and Zn(II) complexes are 43, 56, 62 and 77 µg/ mL, respectively). It is suggested that Cu(II) complex possesses higher scavenging activity towards hydroxyl radical than the parent ligand. The values were found to be close to the values of standard ascorbic acid (IC_{50} value is 22 µg/mL). All other ligands and their metal complexes showed similar behavior.

4.3 Antibacterial activity

The above prepared 2-pyrazolines were assayed for their antimicrobial activities against six test organisms, *Escherichia coli, Staphylococcus aureus, Klebsiella pneumoniae, Proteus mirabillis* and *Salmonella typhii,* at a concentration of 100 mg/mL using the agar well technique [49]. Further, their MIC values against these organisms were determined by serial dilution method using DMSO as a solvent and were compared with streptomycin as

_____

standard antibiotic. DMSO is often recommended to be a vehicle for hydrophobic compounds. In this study, DMSO was used safely with less than 0.15% concentrations. The results obtained are given in Table 2.

Antibacterial activity of the compounds were assessed by the MIC determination and showed order of activity as follows:

CuL > NiL > CoL > ZnL > L

It is indicated that the complex formation was accompanied by the enhancement of activity. Generally, the complexation of the ligand with dipositive metal ions leads to increase in lipophilicity. Further, chelation reduces polarity of metal ion due to partial sharing of its positive charge with donor groups in complexes. This process increased the lipophilicity of metal complexes and thereby, facilitated their permeation through the lipid bilayer of candidal membranes [50]. The enhanced growth inhibition activity of the synthesized metal complexes when compared to their ligands might be due to their chelating ability. The redox behavior of the copper ion in the complexes might also add to the higher anti-microbial activity. The results from these studies could pave the way for the development of next generation antibiotics for therapeutic use.

The higher activity of the copper(II) complex with respect to the nickel(II) complex might be attributed to the higher lipophilicity of the former as compared to the latter as a result of the lower charge density of the copper(II) in copper complex as compared to nickel(II) in the nickel complex.

Antituberculosis activities
The anti-tubercular activity studies of metal complexes of pyrazoline derivatives (Table 3), the ligands with electron withdrawing group (-Nitro substituent) have exhibited excellent inhibition with MIC (Minimum Inhibitory Concentration) less than 10 µg/mL. The ligand L^2 with -CH$_3$ substituent, acts as electron donating group showed moderate activity at 25 µg/ml as compared to standards used viz., streptomycin (7.5 µg/ml) and pyrazinamide (10 µg/ml), respectively. It was observed from the MIC values in Table 4, a change in the substituent on the phenylhydrazine core alters both the activity and selectivity of the pyrazoline derivatives. The remarkable decrease in potency was observed when the unsubstituted phenylhydrazine structural core was replaced by electron donating 2,3-dimethylphenylhydrazine, while the activity was enhanced when 3-nitrophenylhydrazine substitution was executed.

The log P (hydrophobicity of the compound) plays an important role in the penetration through *M. tuberculosis* cell wall and its relationship with antitubercular activity. In the present investigations, the ligand L^3 has observed the log P (3.82) in between 3 and 5 which is ideal for penetration through mycobacterial cell, while other compounds have more than 5.

SOD activity
Superoxide anions have a very short half life and produced continuously. In this colorimetric based assay, Inhibition of the reduction of nitroblue tetrazolium (NBT) to formazan (F) by the reported metal(II) complexes was used for detection of the SOD mimetic catalytic activity of these chelates in the phosphate buffer under similar biological conditions. As the reaction proceeding, the farmazan color is developed and the color changes from colorless to blue, which was associated with an increase in the absorbance at 560 nm. SOD reduces the superoxide ion concentration and thereby lowers the rate of formazan formation. In the SOD-like activity test, the metal complexes compete with NBT for oxidation of the generated superoxide ions. The more efficient the complex, the lower the concentration that corresponds to 50% inhibition of NBT reduction; this concentration is termed IC$_{50}$ for comparative purposes. Figure 5 shows the percentage of inhibiting NBT reduction with an increase in the concentration of the metal complexes of L^1.

The data in Table 4 also reports the scavenging efficiency of each complex, giving its final concentration that produced efficient quenching of the superoxide anion radical. It also reveals that there are difference between the values of scavenging effectiveness and the catalytic constant of the complexes. This difference in the reactivates of these complexes can rationalized by means of correlation between the redox potential of the couples Cu^{II}/Cu^{I} during the catalytic cycle and the SOD-mimetic activity.

The higher biological activities of copper complexes may be attributed to the flexible ligands, which are able to accommodate the geometrical change from Cu^{II} to Cu^{I}, specially the labile water molecules, which are proposed to be easily substituted by the substrate $O_2^{\cdot-}$, in the catalytic process, just like the $O_2^{\cdot-}$, in place of H_2O bound to copper site in the mechanism of dismutation of $O_2^{\cdot-}$ by native SOD. The mechanism proposed for the dismutation of

_____

superoxide anions by both superoxide dismutase and complexes 2 and 3 is thought to involve redox cycling of metal(II) ions (eqs. 1 and 2):

$$M^{2+} + O_2^- \quad \rightarrow M^+ \ + \ O_2$$
$$M^+ + O_2^- + 2H^+ \quad \rightarrow M^+ \ + \ H_2O_2$$
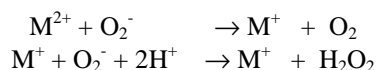
It has been proposed that electron transfer between copper(II) and superoxide anion radicals occurs through direct binding. Therefore, copper complexes exhibited higher SOD activity than other metal complexes. This observation was confirmed by distortion of geometry ("f" factor value). The synthesized copper complexes have higher distortion of geometry.

1-acetyl-2-hydroxynaphthalene

imidazole-2-carbaldehyde

Where
X = -H (L^1), -2,3-dimethyl (L^2), 3-nitro (L^3)
M = Cu(II), Co(II), Ni(II) & Zn(II)
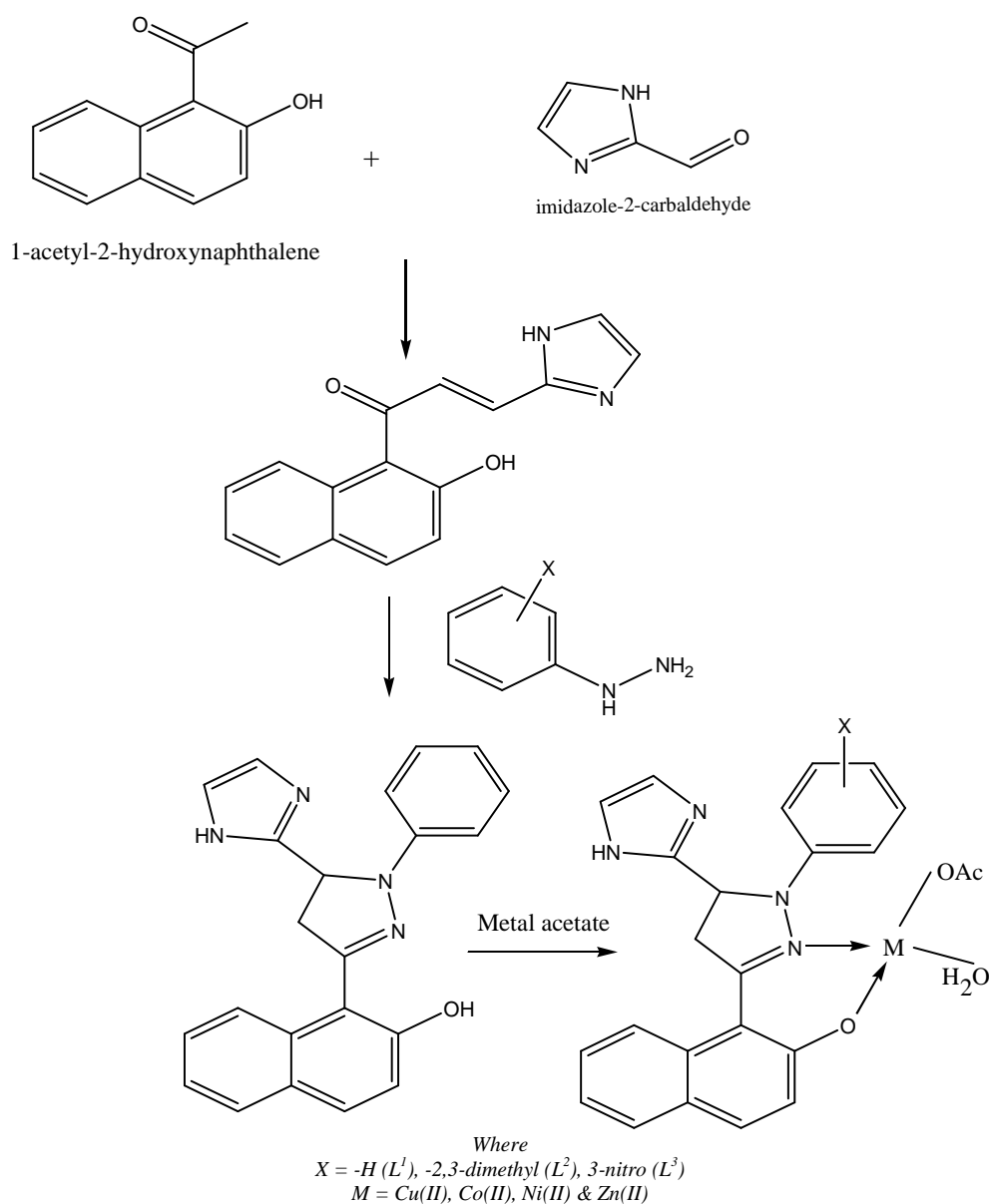
Scheme 1 The schematic outline for the synthesis of metal complexes with prazoline derivatives

_____

Imidzole moiety responsible for enhncement
of biological activities

chemical modification decides biological
activities

Top

Pyrzoline moiety -
important
heterocycle
for biological
activities

OH

bottom
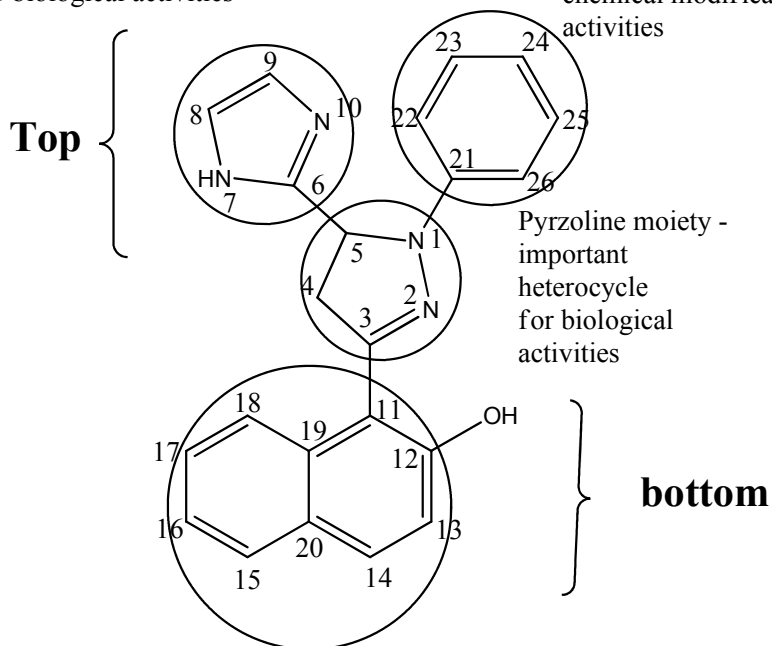
chemical modification decides biological
activities

Figure 1 Structural modification to obtain bioactive lead molecules
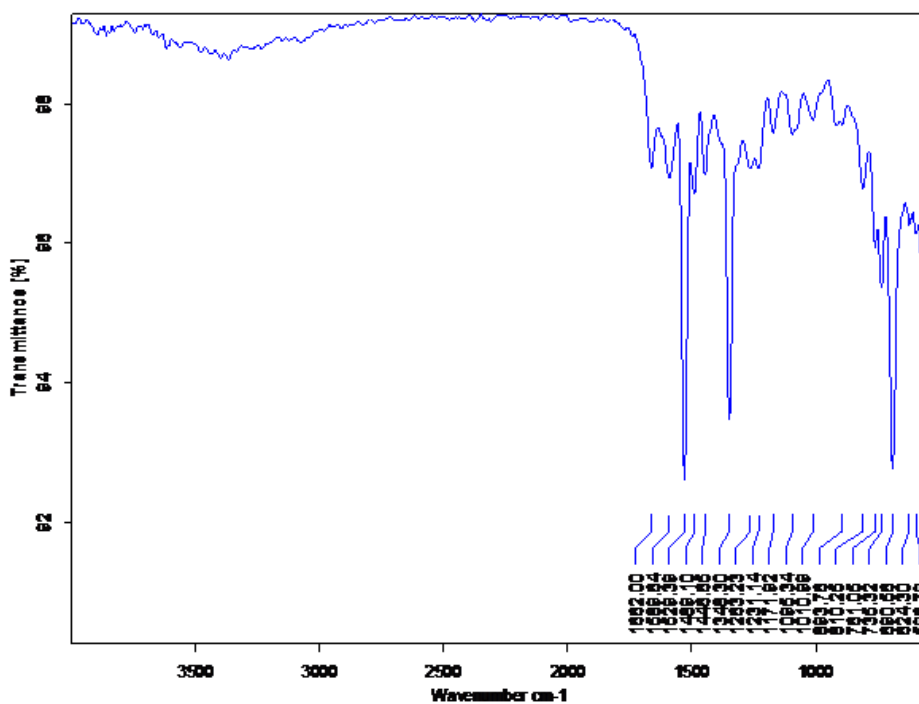

Figure 2   IR spectrum of copper complex of L[1]
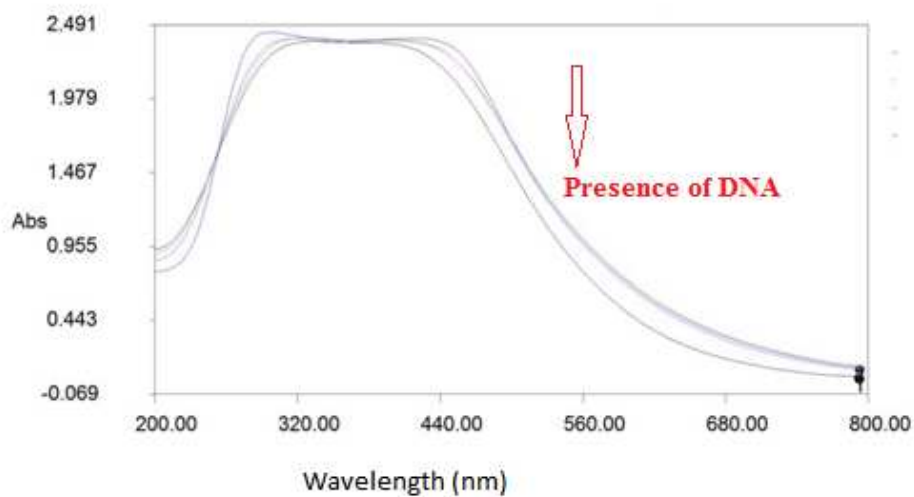
Figure 3   **DNA binding study of copper complex of L[1]**
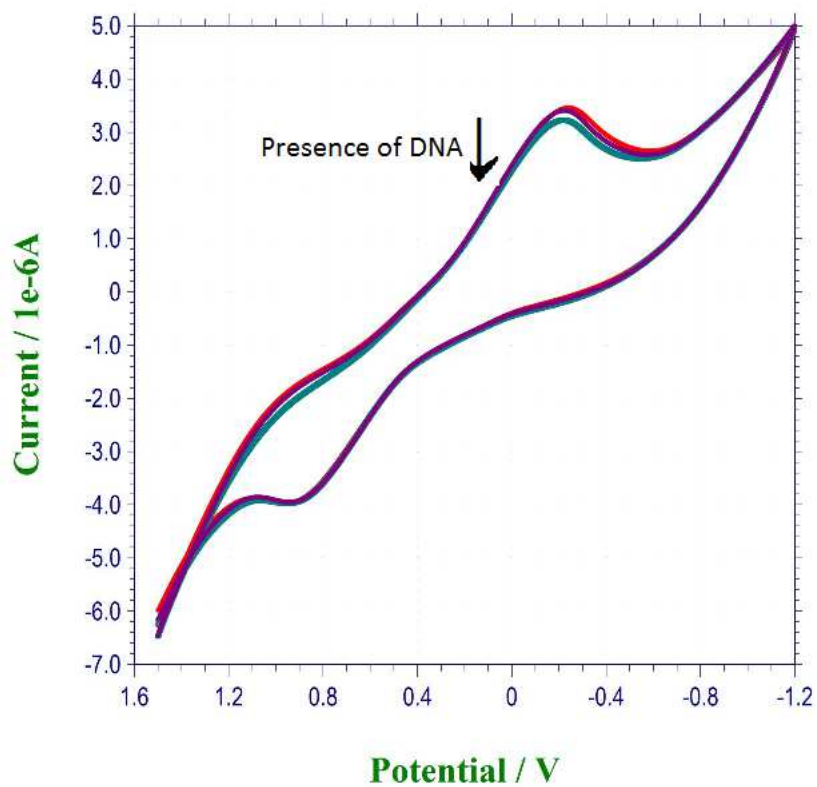
Figure 4   **DNA binding study of copper complex of L[1]**

_____
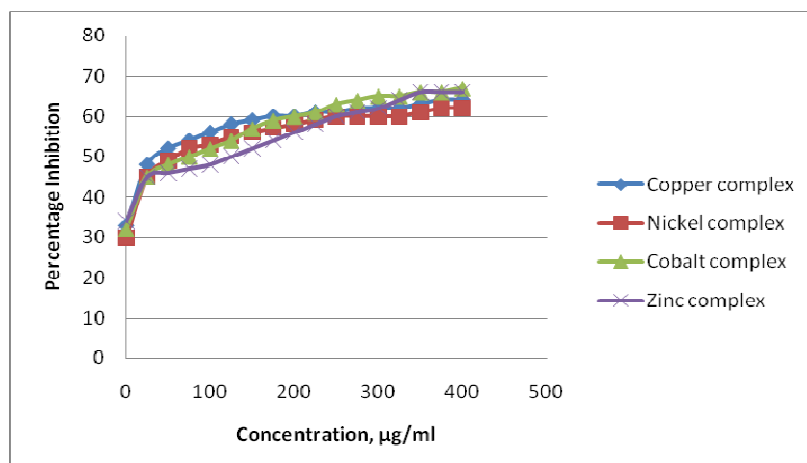
Figure 5   SOD activity of metal complexes of L¹

Table 1 Antioxidant activity of metal complexes

Compound	$IC_{50}(\mu mol\ dm^{-3})$ H_2O_2	$IC_{50}(\mu mol\ dm^{-3})$ $O_2^{\bullet-}$
$[CuL^1(OAc)_2]$	43	40
$[CuL^2(OAc)_2]$	36	30
$[CuL^3(OAc)_2]$	38	37
Ascorbic acid	22	18

Table 2   Antibacterial of ligands and their metal complexes

Compounds	MIC values (µg/ mL)				
	E. coli	*S. aureus*	*K. pneumonae*	*S. typhii*	*P. mirabilis*
L^1	88	76	66	90	94
L^2	76	68	88	60	82
L^3	82	70	76	68	88
$[CuL^1(OAc)(H_2O)]$	36	42	28	40	46
$[CoL^1(OAc)(H_2O)]$	66	54	62	70	50
$[NiL^1(OAc)(H_2O)]$	50	48	50	54	62
$[ZnL^1(OAc)(H_2O)]$	56	62	70	66	52
$[CuL^2(OAc)(H_2O)]$	50	42	28	40	46
$[CoL^2(OAc)(H_2O)]$	54	56	42	48	64
$[NiL^2(OAc)(H_2O)]$	60	48	40	52	72
$[ZnL^2(OAc)(H_2O)]$	72	66	50	46	56
$[CuL^3(OAc)(H_2O)]$	36	42	28	40	46
$[CoL^3(OAc)(H_2O)]$	50	56	46	52	64
$[NiL^3(OAc)(H_2O)]$	44	64	48	52	60
$[ZnL^3(OAc)(H_2O)]$	40	66	44	62	56
Streptomycin	10	18	20	16	14

Table 3 Anti-tuberculosis activity of the effective metal complexes

Sl.No	Effective metal complexes	MIC values (µM)
1	$[CuL^1(OAc)\ (H_2O)]$	4
2	$[CuL^2(OAc)\ (H_2O)]$	8
3	$[CuL^3(OAc)\ (H_2O)]$	6
4	native bovine erythrocyte	0.04

Table 4 SOD activity of effective metal complexes

Sl.No	Effective metal complexes	IC_{50} values (µg/mL)
1	$[CuL^1(OAc)(H_2O)]$	14.6
2	$[CuL^2(OAc)(H_2O)]$	11.2
3	$[CuL^3(OAc)(H_2O)]$	15.8
4	Streptomycin	7.5
5	Pyrazinamide	10

_____

CONCLUSION

In the present work attempts, to rationalize the Quantitative structure–activity relationship of metal complexes of pyrazoline scaffold for antituberculosis agent. The design and synthetic approach was concentrated on the development of of metal complexes of pyrazoline analogue with improved anti-tuberculosis activity. The Claisen Schmidt condensation of 1-acetyl-2-hydroxynaphathalene with imidazole-3-carboxaldehyde in presence of sodium hydroxide resulted into the formation of chalcone. The chalcone underwent sodium hydroxide assisted cyclization with substituted phenylhydrazines to form ligand (L^1-L^3). Cobalt, nickel, copper and zinc complexes of the synthesized ligands were synthesized (scheme 1). The lower molar conductance values of the complexes which corresponds to non-electrolytic nature. The observed anti tuberculosis assay screening showed that higher potencies of copper complexes of pyrazoline derivatives as compared with other metal complexes. The improved potencies of copper complexes with pyrazoline derivatives reported here to open up new opportunities for synthesizing different derivatives around 'pyrazoline' scaffold as anti-tuberculosis agents. On the basis of the above observations, modification will be done to improve antimycobacterial activity. *In vivo* studies of the complexes are in progress in order to understand the variation in their biological effects, which could be helpful in designing more potent anti-tuberculosis agents for therapeutic use.

REFERENCES

[1] S. Sathiyaraj, K.Sampath, R.J.Butcher, R. Pallepogu, C.Jayabalakrishnan, *Eur. J. Med. Chem.*, 64 (**2013**) 81-89.
[2] R.B.Weiss, M.C.Christian, *Drugs*, 46 (**1993**) 360–377.
[3] J.J.Criado, J.L.Manzano, E.Rodriguez-Fernandez, *J Inorg Biochem.*, 96 (**2003**) 311–320.
[4] E.Wong, C.M.Giandomenico, *Chem Rev.*, 99 (**1999**) 2451–2466.
[5] Y.P.Ho, S.C.Au-Yeung, *Med Res Rev.* 23 (**2003**) 633–655.
[6] C.Marzano, M.Pellei, F.Tisato, C.Santini, *Agents Med. Chem.*, 9 (**2014**) 185–211.
[7] L.Ruiz-Azuara, M.E.Bravo-Gomez, *Curr. Med. Chem.* 17 (**2010**) 3606–3615.
[8] A.E.E. Amr, H.H. Sayed, M.M. Abdulla*, Arch. Pharm.*, 338 (**2005**) 433–440
[9] J.C. Jung, E. Blake Watkins, M.A. Avery, *Heterocycles,* 65 (**2005**) 77–94
[10] E. Palaska, M. Aytemir, I. Tayfun Uzbay, D. Erol, *Eur. J. Med. Chem.*, 36 (**2001**) 539–543
[11] E. Bansal, V.K. Srivastava, A. Kumar, *Eur. J. Med. Chem.*, 36 (**2001**) 81–92.
[12] E. Palaska, D. Erol, R. Demirdamar, *Eur J Med Chem*, 31 (**1996**) 43.
[13] M. Abid, A. Azam, *Eur J Med Chem*, 40 (**2005**) 935.
[14] T.Eicher, S. Hauptmann, Edition IInd, 'The Chemistry of Heterocycles: Structure, Reactions, Syntheses, and Applications', Wiley-VCH (**2003**).
[15] T. Eicher, S. Hauptmann, The Chemistry of Heterocycles, Structures, Reactions, Synthesis and Applications, Wiley-VCH GmbH & Co. KGaA, Weinheim (**2006**).
[16] F. Rondu, S. Le Bihan, G.X. Wang, A. Lamouri, E. Touboul, G. Dive, T. Bellahsene, B. Pfeiffer, P. Renard, B. Guardiola-Lemaitre, D. Manechez, L. Penicaud, A. Ktorza, J.J. Godfroid, *J. Med. Chem.* 40 (**1997**) 3793.
[17] A.M. Venkatesan, A. Agarwal, T. Abe, H.O. Ushirogochi, D. Santos, Z. Li, G. Francisco, Y.I. Lin, P.J. Peterson, Y. Yang, W.J. Weiss, D.M. Shales, T.S. Mansour, *Bioorg. Med. Chem.* 16 (**2008**) 1890
[18] S. Schwoch, W. Kramer, R. Neidlein, H. Suschitzky, *Helv. Chim. Acta* 77 (**1994**) 2175.
[19] T.H. Fife, *Acc. Chem. Res.* 26 (**1993**) 325.
[20] V.G. Desai, P.C. Satardekar, S. Polo, K. Dhumaskar, *Synth. Commun.*, 42 (**2012**) 836–842.
[21] Shamsuzzaman, M.S. Khan, M. Alam*, J. Chil. Chem. Soc.,* 54 (**2009**), pp. 372–374.
[22] W.J. Geary, *Coord. Chem. Rev.,* 7 (**1971**) 81.
[23] M.Kuriakose, MRP Kurup, E. Suresh, *Spectrochim Acta. Mol Biomol Spectrosc.* 66(2) (**2007**) 353-358.
[24] D. Prakash, C. Kumar, S. Prakash, A. K. Gupta, and K. R. R. P. Singh*, Journal of the Indian Chemical Society*, 86(12) (**2009**) 1257–1261.
[25] K. Nakamoto, Infrared Spectra of Inorganic and Coordination Compounds", Wiely, New York (**1970**).
[26] A. B. P. Lever. `Inorganic Electronic Spectroscopy', P. 333, Elsevier, Publishing Co., New York (**1968**).
[27] Alzheimer's disease facts and figures. *Alzheimers Dement.*, 5(3) (**2009**) 234–270.
[28] P.K. Ray, B. Kauffman. *Inorg. Chim. Acta.* 173 (**1990**) 207.
[29] C.C.Curtain, F.Ali, I.Volitakis, R.A.Cherny, R.S.Norton, K.Beyreuther, C.J.Barrow, C.L.Masters, A.I.Bush, K.J.Barnham*, J. Biol. Chem.*, 276(23) (**2001**) 20466–20473.
[30] J.Dong, C.S.Atwood, V.E.Anderson, S.L.Siedlak, M.A.Smith, G.Perry, P.R.Carey, *Biochemistry.* 42(10) (**2003**) 2768–2773.

_____

[31] C. Opazo, X.Huang, R.A.Cherny, R.D.Moir, A.E.Roher, A.R.White, R.Cappai, C.L.Masters, R.E.Tanzi, N.C.Inestrosa, A.I.Bush, *J. Biol. Chem*., 277(43) (**2002**) 40302–40308.

[32] X.Huang, C.S.Atwood, M.A.Hartshorn, G.Multhaup, L.E.Goldstein, R.C.Scarpa, M.P.Cuajungco, D.N.Gray, J.Lim, R.D.Moir, R.E.Tanzi, A.I.Bush, *Biochemistry*. 38(24) (**1999**) 7609–7616.

[33] Mamta Rani, Mohamad Yusuf, Salman Ahmad Khan, P.P. Sahota, G. Pandove, *Arabian J. Chem*., 8 (**2015**) 174–180.

[34] G. G. Kondrat'eva, M. N. Volkotrub, Sin. Issled, Eff.Khim Dobavok., *Polim. Mater*. 2 (**1969**) 373 – 376.

[35] K. J. Liska, *J. Med. Chem*.15 (**1972**) 1177.

[36] H. Harada, M. Usui, Jpn Patent JP 62, 111 (**1985**) 988.

[37] D. W. Clayton, W. E. Elstow, R. Ghosh , B. C. Platt, *J. Chem. Soc*. (**1953**) 581.

[38] Pathan H. Aishakhanam, Bakale P. Raghavendra, Naik N. Ganesh, Frampton S. Christopher, Gudasi B. Kalagouda, *Polyhedron* 34 (**2012**) 149.

[39] N. Raman, A. Selvan. P. Manissankar. *Spectrochim. Acta*. A 76 (**2010**) 161.

[40] E.M. Tuite, J.M. Kelley, *Biopolymers* 35 (**1995**) 419–433.

[41] J.M. Kelley, W.J.M. Van der Putten, D. McConnell, *J. Photochem. Photobiol*. 45 (**1987**) 167–175.

[42] W.J.M. Van der Putten, J.M. Kelley, *Photochem. Photobiol*. 49 (**1989**) 145–151.

[43] Q. S. Li, P.Yang, H.F.Wang, M.L.Guo, *J. Inorg. Biochem*., 64 (**1996**) 181-195.

[44] S.Shi, J.Liu, J.Li, K.C.Zheng, X.M.Huang, C.P.Tan, L.M.Chen, L.J. Ji, *J. Inorg. Biochem*., 100 (**2006**) 385-395.

[45] G. Paillard, R. Lavery, Analyzing protein-DNA recognition mechanisms, *Structure*, 12 (**2004**) 113–122.

[46] A. Łęczkowskaa and R. Vilara, *Annu. Rep. Prog. Chem., Sect. A: Inorg. Chem., 108* (**2012**) 330-349

[47] M.T. Carter, A.J. Bard, *J. Am. Chem. Soc*. 109 (**1987**) 7528-7530.

[48] S.R.Kannat, R. Chander, A.Sharma, *Food Chemistry*, 100 (**2007**) 451-458.

[49] S. Magaldi, S. Mata-Essayag, C. Hartung de Capriles, C. Perez, M.T Colella, Carolina Olaizola, Yudith Ontiveros, *Int. J. Infectious Diseases*, 8 (**2004**) 39–45.

[50] S.U.Rehman, Z.H.Chohan, F.Gulnaz, C.T.Supuran, *J. Enz. Inhib. Med. Chem*., 20(4) (**2005**) 333-340.

[51] Y. Ishibashi, M.Fujiwara, T.Umesato, H.Saito, S.Kobatake, M.Irie, H.Miyasaka, *J. Phys. Chem*. C 115 (**2011**) 4265–4272.

[52] C.Yun, J.You, J. Kim, J. Huh, E.Kim, *J. Photoch. Photobiol. C Photochem. Rev*. 10 (**2009**) 111–129.

[53] M. Ashraf, G.J. Gainsford, A.J.Kay, *Aust. J. Chem*., 65 (**2012**) 779–784.

[54] P.D.Patel, A.E. Masunov, *J. Phys. Chem*. C, 115 (**2011**) 10292–10297.

[55] P.D.Patel, A.E. Masunov, *J. Phys. Chem*. A 113 (**2009**) 8409–8414.

[56] D.Jacquemin, E.A. Perpete, F. Maurel, A.Perrier, *J. Phys. Chem*. C, 114 (**2010**) 9489–9497.

[57] J.C. Crano, T.Flood, D.Knowles, A.Kumar, B.Van Gemert, *Pure Appl. Chem*. 68 (**1996**) 1395–1398.

[58] A.S.Dvornikov, J. Malkin, P.M.Rentzepis, *J. Phys. Chem*. 98 (**1994**) 6746–6752.

[59] I.Willner, S.Rubin, R.Shatzmiller, T.Zor, *J. Am. Chem. Soc*., 115 (**1993**) 8690–8694.

[60] J.D.Winkler, K.Deshayes, B.Shao, *J. Am. Chem. Soc*., 111 (**1989**) 769–770.